Transient biphotonic holographic grating in photoisomerizative azo materials

Pengfei Wu,* Li Wang, Jiren Xu, and Bingsuo Zou†
Laboratory of Optical Physics, Institute of Physics, Chinese Academy of Sciences, P.O. Box 603, Beijing 100080, China

Xiong Gong, Guilan Zhang, Guoqing Tang, and Wenju Chen
Institute of Modern Optics, Nankai University, Tianjin 300071, China

Wei Huang
Institute of Materials Research and Engineering, National University of Singapore, Singapore 119260, Singapore
(Received 23 July 1997)

Transient grating of biphotonic holography is studied theoretically and experimentally in *trans-cis* isomerization azo materials. The theoretical description of the transient biphotonic holographic grating agrees well with experimental results in methyl yellow-polymethylmethacrylate and ethyl orange-polyvinylalcohol films. The mechanism of the biphotonic holographic grating in the azo materials can be attributed to the redistribution of *cis* isomers induced by both the short-wavelength light and the long-wavelength light, which is confirmed by the experimental results of polarized biphotonic holography. [S0163-1829(98)11003-2]

I. INTRODUCTION

There has been a wide scientific interest in photoisomerizative organic materials for the studies on nonlinear optics and photonics applications in recent decades.[1] Azo dyes, which possess *trans-cis* isomerization property under irradiation at an appropriate wavelength, are among the most attractive photoisomerizative materials due to their high inherent optical nonlinearities and their abundant nonlinear optical behaviors.[2] These materials are commonly incorporated either as guests into different hosts (polymer, liquid crystal)[3–5] or as pendant side groups on the polymer main chains[6–8] to form various dye-host systems in order to improve their optical properties and investigate their suitability for the applications in photonic devices. By selecting or tailoring both the dyes and the host molecules, the dye-host systems can be optimized to the desired effect.[9] Many nonlinear behaviors were observed in these dye-host systems and many nonlinear optical techniques, such as degenerate four wave mixing,[10,11] attenuated total reflection (ATR) experiment,[12] photorefractive[13] and photoinduced anisotropy measurement,[14] have been used to elucidate the contribution of azo molecules to the nonlinear effects.

Since holographic gratings have potential applications for information storage,[15,16] waveguide coupling,[17] and optoelectronics,[18] a large fraction of the studies on azo materials involved in the holographic gratings and considerable progress have been achieved in this field. The formation of the holographic gratings in the azo materials are mainly a result of the resonance absorption of the dye molecules,[10] *trans-cis* photoisomerization,[19] or the photoinduced reorientation of *trans* form molecules.[17,20,21] The last mechanism is predominant in the case of the azo chromophores with strongly interacting groups (donor, acceptor) that contribute to the increase in both the second-order and the third-order optical nonlinearities.[22,23] The reorientation process involves the repeated $trans \rightarrow cis$ photoisomerization of the azo chromophores and the thermal $cis \rightarrow trans$ relaxation, resulting in the alignment of the *trans* azo molecular axes in the direction perpendicular to the polarization of incident light.[24] Therefore, the reorientation gratings depend on the polarization of writing interference field. Unlike the resonance absorption grating and the photoisomerizative grating, the photoinduced reorientation gratings have a very long lifetime, even up to several years,[25] after the exciting lights are turned off. Recently, another kind of holographic grating, surface relief grating,[26–28] was observed in many azo polymers by atomic force microscopy. This grating is formed on the surface of a sample and shows a very regularly spaced surface relief structure and does not require any chemical resistance processing. The profile height of the surface grating near 900 nm and the diffraction efficiency of over 42% have been obtained in an azo polymer film by Barrett, Natansohn, and Rochon.[29] Some researchers believe that mass transport plays a role in the formation of the surface grating; however, their mechanism is not very clear at present.

In general, most of the azo molecules undergo isomerization, reorientation, and mass transport only with absorbing a blue or green light, which is commonly provided by bulky laser equipment, such as an Ar^+ laser. This limits the application of these materials for photonic devices, especially for integrated optical elements. In this paper, we present a type of grating formation process in azo/polymer films, which operates under two color lights, a short-wavelength noncoherent light from Hg light source and a long-wavelength coherent light from a HeNe laser. With this biphotonic method the recording wavelengths can be extended to about 600 nm and upwards, where most miniature diode lasers can be used. Moreover, the experimental results of the biphotonic grating could lead to a better understanding of the photoisomerization mechanism of the azo molecules.

II. THEORETICAL MODEL

It is well known that the azo dyes have the isomerization property under light irradiation and heating. Usually two

kinds of isomers, *trans* and *cis*, are involved in the isomerization process for most of the azo molecules, especially the two-ring azobenzene (mono-azobenzene) derivatives; although some macro azo molecules such as bi-azo molecules may produce intermediate isomer (or intermediate product), which is thermally unstable and isomerizes easily to the other two isomers.[30] The *trans* isomer and the *cis* isomer have different absorption spectra resulting from their different structures. The *trans* isomers are much more stable than *cis* isomers in natural condition and most azo molecules exist in this form.[31] Therefore, the linear absorption spectrum of azo molecules mainly shows the absorption features of the *trans* isomers and mostly lies in the short-wavelength regions (blue-green light and uv). When the *trans* isomers absorb the short-wavelength light, they isomerize to the *cis* form and the maximum of visible absorption band changes. In our experiments presented below, an absorption redshift is obtained. It is suggested that the *cis* isomers of the azo dye in polymer films continually absorb the long-wavelength light and return to the *trans* form. Also, the *cis* isomers can isomerize back to the *trans* form through thermal process. The isomerization process of the azo dyes can be simply represented as follows:

$$trans \underset{R_2,R_T}{\overset{R_1}{\rightleftarrows}} cis,$$

where R_i is the rate of the photoisomerization, $i=1,2$ corresponding to the photoisomerizations from *trans* to *cis* and from *cis* to *trans*, respectively. R_T is the rate of the thermal isomerization from *cis* to *trans*. Based on this model, when both the short-wavelength and the long-wavelength lights irradiate the azo molecules, we can describe the isomerization rate equation as

$$\dot{N}_1(t) = -R_1 N_1(t) + (R_2 + R_T) N_2(t), \tag{1}$$

where $N_1(t)$ and $N_2(t)$ are the populations of the *trans* isomer and the *cis* isomer, respectively. By a straightforward calculation, we obtain

$$N_1(t) = \frac{(R_2+R_T)N_0}{R_1+R_2+R_T}\left\{1+\frac{R_1}{R_2+R_T} \times \exp\left[-(R_1+R_2+R_T)t\right]\right\},$$

$$N_2(t) = \frac{R_1 N_0}{R_1+R_2+R_T}\{1-\exp\left[-(R_1+R_2+R_T)t\right]\}, \tag{2}$$

where N_0 is the total population of the azo molecules, i.e., $N_0 = N_1(t) + N_2(t)$. In the arrangement of biphotonic holographic experiment described in Sec. IV, the irradiation of the short-wavelength light is noncoherent and uniform on the sample, so the *trans* isomers are isomerized uniformly to the *cis* isomers in space by the short-wavelength light. The long-wavelength light comes from a coherent laser, which is first divided into two beams and then are incident onto the azo sample in a suitable angle. Due to the spatial intensity modulation induced by the interference of the two long-wavelength beams in the sample, the photoisomerization from *cis* to *trans* is spatially modulated. As a result, the population of the *cis* isomers is also modulated in the azo sample, which forms a population grating. The modulated contrast of the *cis* population grating is described by

$$\Delta N_2(t) = \left(\frac{\partial N_2(t)}{\partial I_2}\right)\Delta I_2, \tag{3}$$

I_1 and I_2 are the intensities of the short-wavelength light and the long-wavelength light, respectively; ΔI_2 is the modulated contrast in the interference field of the long-wavelength light. The diffraction efficiency of the grating is proportional to the square of the modulated contrast $\Delta N_2(t)$. The photoisomerizative rate of R_i is related to the incident intensity of I_i (Ref. 32) as $R_i = \sigma_i \phi_i I_i / \hbar \omega_i$, where σ_i is the absorption cross section of the *trans* ($i=1$) or the *cis* ($i=2$) isomer, ϕ_i is the quantum yield of the photoisomerization from *trans* to *cis* ($i=1$) or from *cis* to *trans* ($i=2$), and ω_i is the angular frequency of the short-wavelength ($i=1$) or the long-wavelength ($i=1$) light. R_T is a constant at a definite sample temperature. We define $R_i/R_T = A_i I_i$, where $A_i = \sigma_i \phi_i / \hbar \omega_i R_T$, which is determined by the exciting wavelength and the molecular characters of the *trans* form and the *cis* form. For the different azo molecules, their A_i's are different. From Eqs. (2) and (3), one can derive

$$\Delta N_2(t) = \frac{-A_1 A_2 I_1 I_2 N_0}{(1+A_1 I_1 + A_2 I_2)^2}\{1-[1+(1+A_1 I_1 + A_2 I_2)R_T t]\exp[-(1+A_1 I_1 + A_2 I_2)R_T t]\}. \tag{4}$$

This result describes the temporal behavior of the grating after both the short-wavelength light and the long-wavelength light irradiate the sample. When $t=0$, $\Delta N_2(0)=0$ based on Eq. (4), it means that the grating has not yet formed at the very moment when the two color lights are turned on. With the time increasing ($t>0$), $|\Delta N_2(t)|$ is also monotonically increased. When the time $t \to \infty$,

$$|\Delta N_2(\infty)| \to \frac{A_1 A_2 I_1 I_2 N_0}{(1+A_1 I_1 + A_2 I_2)^2}.$$

The grating contrast reaches its saturation value. The leading parts of curves in Fig. 1(a) ($t=0 \to 0.5/R_T$) and Fig. 1(b) ($t=0 \to 2/R_T$) show the temporal evolutions of the grating $(\Delta N_2)^2$ for the different values of $A_1 I_1$ and $A_2 I_2$ according to Eq. (4). It is found that the saturation value $\Delta N_2^2(\infty)$ of the grating increases with the increase of $A_2 I_2$ and reaches its maximum at either $A_1 I_1 = 8$ or $A_1 I_1 = 2$ when the condition of $A_2 I_2 = 1 + A_1 I_1$ is satisfied. Moreover, Eq. (4) shows that the larger the values of $A_1 I_1$ and $A_2 I_2$, the faster the grating builds up.

From the isomerization model and the above discussion, it is clear that the short-wavelength light has an important effect on the buildup of the biphotonic holographic grating. For the formed grating, it is expected that stopping the irradiation of the short-wavelength light will affect the development of the biphotonic grating.

Assume the biphotonic grating has been formed, i.e., the population of the *cis* form reaches their saturation value $N_2 = R_1 N_0/(R_1+R_2+R_T)$ in the grating region. At this mo-

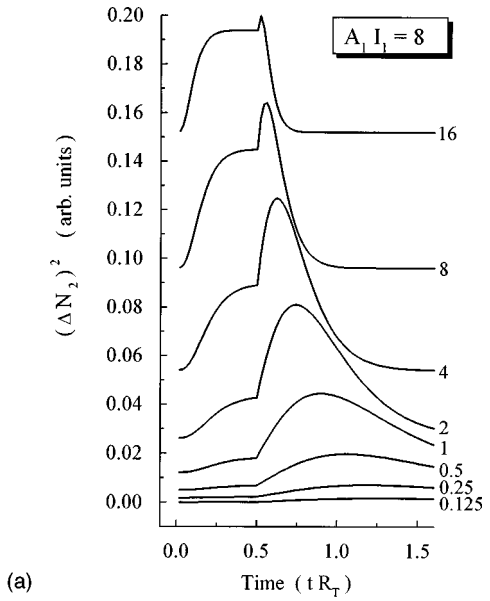

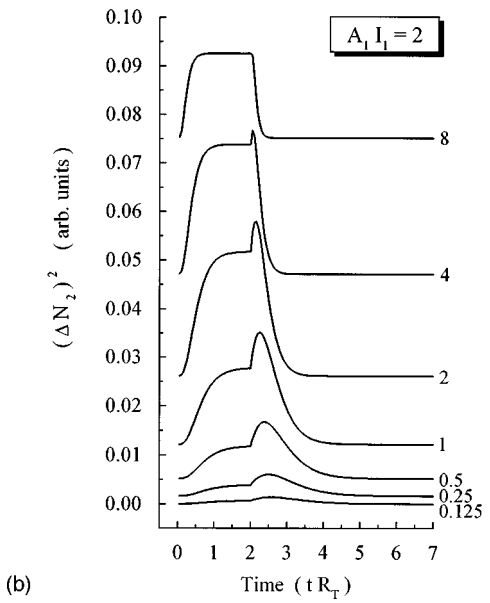

FIG. 1. Theoretical curves of transient biphotonic grating. At $t=0$, both short-wavelength light and long-wavelength light irradiate the azo molecules; at (a) $t=0.5/R_T$, (b) $t=2/R_T$, stopping the irradiation of the short-wavelength light. The curves with different values of A_2I_2 marked by the right side of the curves are offsetted vertically in each case of A_1I_1.

ment, blocking the short-wavelength light (I_1), the isomerization process can be described as follows:

$$\dot{N}_2(t)=-(R_2+R_T)N_2(t), \tag{5}$$

and the solution is

$$N_2(t)=\frac{R_1N_0}{R_1+R_2+R_T}\exp[-(R_2+R_T)t]. \tag{6}$$

Using Eqs. (3) and (6), we obtain

$$\Delta N_2(t)=\frac{-A_1A_2I_1I_2N_0}{(1+A_1I_1+A_2I_2)^2}[1+(1+A_1I_1+A_2I_2)R_Tt]\exp[-(1+A_2I_2)R_Tt], \tag{7}$$

where A_i is the same as defined above. Equation (7) describes the transient variation of the biphotonic holographic grating after the irradiation of the short-wavelength light stops. The latter parts of the curves in Fig. 1(a) ($t\geqslant 0.5/R_T$) and Fig. 1(b) ($t\geqslant 2/R_T$) show the transient behaviors of the gratings for the different values of A_1I_1 and A_2I_2 according to Eq. (7). It is found that removing the short-wavelength light causes the grating not to reduce immediately, but to enhance first and then to decay. The peak of $|\Delta N_2|$ expressed as

$$\frac{A_1A_2I_1I_2N_0}{(1+A_1I_1+A_2I_2)(1+A_2I_2)}\exp\left[\frac{-A_1I_1}{1+A_1I_1+A_2I_2}\right],$$

is obtained at a time of

$$t=\frac{A_1I_1}{(1+A_1I_1+A_2I_2)(1+A_2I_2)R_T}+\frac{0.5}{R_T}$$

for case (a), and

$$t=\frac{A_1I_1}{(1+A_1I_1+A_2I_2)(1+A_2I_2)R_T}+\frac{2}{R_T}$$

for case (b). Therefore, with the increase of A_2I_2, the time for the grating reaching the maximum gets shorter and shorter; from Eq. (7) it also can be seen that the decay of the grating following the maximum gets faster and faster. Moreover, after the value of A_2I_2 increases to a certain value, the peak of the grating will vanish.

III. SAMPLE PREPARATION AND CHARACTERIZATION

Two kinds of mono-azobenzene molecules, methyl yellow (MY, 4-dimethylamino-azobenzene) and ethyl orange (EO, 4-diethylamino-azobenzene-4′-sodium sulfonate) are used in our experiments. Their linear absorption spectra are shown in Fig. 2. It shows a broad absorption band centered around 400 nm for MY molecules and around 460 nm for EO molecules, which are due to the $n\rightarrow\pi^*$ and $\pi\rightarrow\pi^*$ absorptions.[31]

The azo molecules are doped into the two kinds of polymers, polymethylmethacrylate (PMMA) and polyvinylalcohol (PVA), respectively, to produce the samples of MY-PMMA film and EO-PVA film. The preparation procedures of the samples are as follows. First of all, MY and PMMA are dissolved separately in chloroform at about 60 °C, and EO and PVA are dissolved separately in water at about 80 °C. Then, the MY solution and the EO solution are poured into the PMMA solution and the PVA solution, respectively, to form the two kinds of mixing solutions of MY-PMMA and EO-PVA. Both the MY-PMMA and the EO-PVA solutions are stirred for 2 h. Then, the solutions are separately coated onto cleaned quartz slides and allowed to dry slowly in a clean and dry cabinet. It should be noted that volatilizing the solvent too fast may cause the surface of the films to be uneven. The contents of both the MY in PMMA and the EO in PVA are 5% by weight, and the thickness of

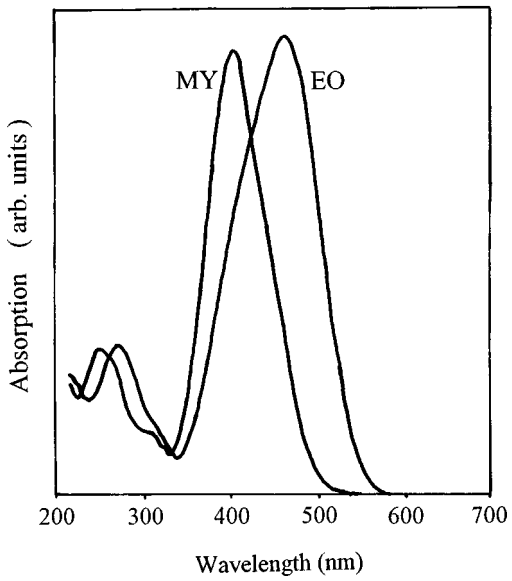

FIG. 2. Linear absorption spectra of MY and EO.

the two films are both about 10 μm.

The $trans \rightarrow cis$ photoisomerization of the azo molecules can be induced by both $n \rightarrow \pi^*$ and $\pi \rightarrow \pi^*$ excitations.[31] In the linear absorption spectra, the incident light intensities are so weak that the photoisomerization of the azo molecules are not obvious. However, if the azo molecules are irradiated by an intense light with wavelength at $n \rightarrow \pi^*$ or $\pi \rightarrow \pi^*$ band, it is expected that the absorption spectra will change, especially in the spectral region of long wavelengths. Figure 3 shows the difference of the transmission spectra with irradiation and without irradiation of the Hg light, which passes through a band-pass filter (350–500 nm) before incident onto the MY-PMMA and the EO-PVA films. The irradiation of blue spectral component in the Hg light causes the samples to absorb light in the long-wavelength regions, where the samples are completely transparent in the absence of the Hg light. The absorption of the MY-PMMA sample can be extended to 660 nm in the spectrum under the irradiation of the Hg light, and for the EO-PVA sample, the extended wavelength of the absorption reaches beyond 750 nm. The declines of the transmission in the long-wavelength regions are due to the absorption of the *cis* isomers, of which the population increases upon the irradiation of the Hg light in both MY and EO molecules.

IV. EXPERIMENTAL RESULTS AND DISCUSSIONS

A. Dynamic behaviors of biphotonic holography

We now present and discuss the results of the biphotonic holographic grating formed in the azo/polymer films. These gratings are erasable and distinguished from other gratings in the azo materials, such as the photoinduced reorientation grating and the surface relief grating, which are formed by one photon excitation close to the center of the absorption band.

The experimental geometry used for the biphotonic holography is schematically drawn in Fig. 4. I_1 is the short-wavelength light that comes from a Hg lamp. After passing through a bandpass filter with the transmission wavelength

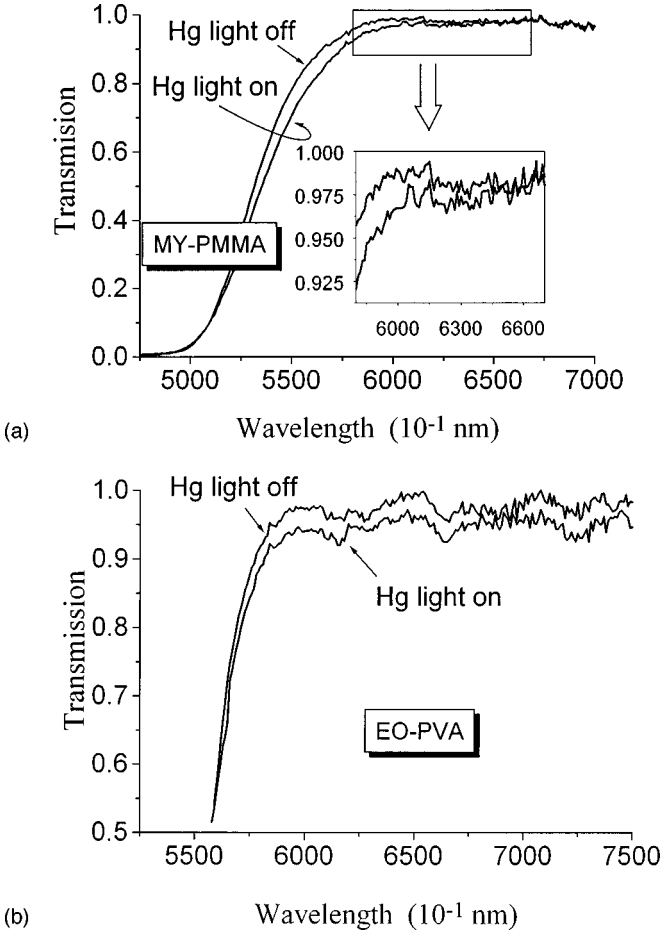

FIG. 3. Transmission spectra with irradiation and without irradiation of Hg light in (a) MY-PMMA film and (b) EO-PVA film.

from 350 nm to 500 nm, the Hg light is focused onto the sample. The long-wavelength lights of I_a and I_b come from a 633-nm HeNe laser and both have *s* polarization. The two beams meet and interfere with each other in the same region of the sample as irradiated by the Hg light. The biphotonic grating is read by another 633-nm HeNe laser (I_c) that counterpropagates with the beam I_a. The induced diffraction signal (I_s) propagates again the beam I_b.

Figure 5 shows the diffraction signals versus time with the different intensities of 633-nm beam from MY-PMMA film and EO-PVA film. The experimental results are in good agreement with the theoretical descriptions on the transient biphotonic grating formation and development in Sec. II, where the two values of $A_1 I_1$ (i.e., two different values of A_1 for the same I_1) characterize the two samples and the different values of $A_2 I_2$ describe the variation of the intensity I_2

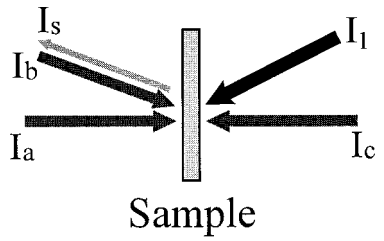

FIG. 4. Experimental geometry used in biphotonic holography.

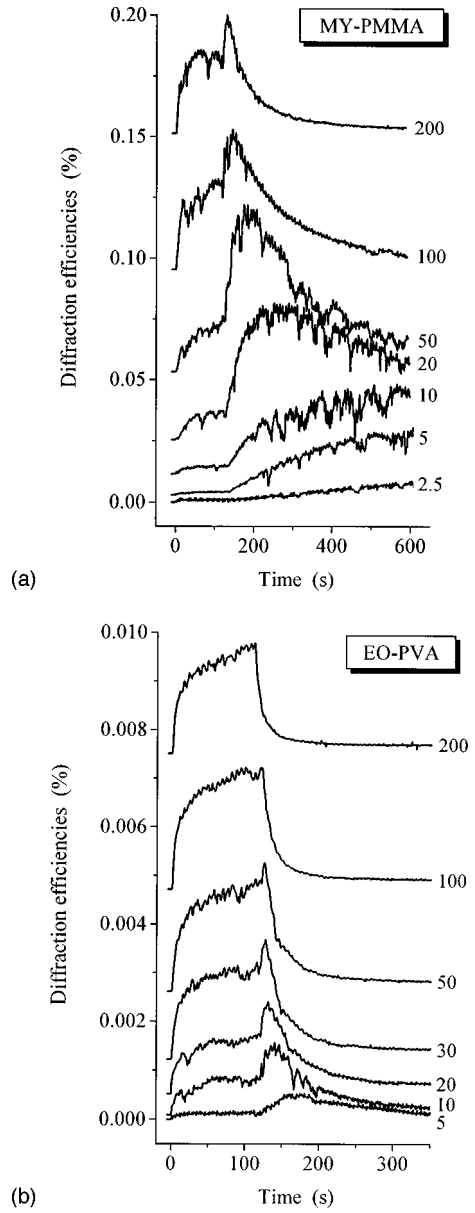

FIG. 5. Transient diffraction efficiencies of biphotonic holography under different 633-nm beam intensities in (a) MY-PMMA film and (b) EO-PVA film. At $t=0$, both 633-nm light and Hg light are turned on; at $t=120$ s, the Hg light is turned off. The signal curves are offsetted vertically according to different 633-nm beam intensities marked by the curves.

for the same sample (i.e., same A_2). In the experiment, the intensity of the Hg light on the film is 8 mW/cm^2; and the three 633-nm beams have equal intensities, which are marked by the side of the curves.

At $t=0$, both Hg light and HeNe beams are simultaneously turned on, the diffraction signals emerge and monotonically increase to their saturations. These saturated diffractions have a maximum when the 633-nm beam intensity is varied. According to the theoretical result, the maximum of the saturated diffraction should satisfy the condition of $A_2 I_2 = 1 + A_1 I_1$, where I_1 corresponds to the intensity of the Hg light and I_2 corresponds to the intensity of each 633-nm beam. This condition establishes a relation between the molecular character A_i for the *trans* isomer and the *cis* isomer. In the experiment, the intensity of the Hg light remains constant but the intensities of the 633-nm light are varied. The maximum of the saturated diffractions occurs at the 633-nm beam intensity of about 150 mW/cm^2 for the MY-PMMA sample and about 100 mW/cm^2 for the EO-PVA sample. Therefore, by measuring the maximum of the saturated diffraction efficiency of the biphotonic holography, the information about the *trans* and the *cis* molecular characters can be obtained, which may be useful in understanding the isomerization mechanism of the azo molecules.

At $t=120$ s when the diffraction signals increase near to saturation in both cases of the MY-PMMA and the EO-PVA samples, the Hg light is blocked. The experimental results show that the signals grow up once again and then decay slowly for both samples. As the 633-nm light intensity increases, the growth and the decay of the diffractive signals become fast, i.e., the diffractive peaks after blocking the Hg light get narrower and narrower, as predicted by the theoretical description. Moreover, with the intensity variation of the 633-nm light, the height of the diffractive peaks after the saturation shows a maximum which emerges at the 633-nm light intensity of about 20 mW/cm^2 for the MY-PMMA sample and at about 10 mW/cm^2 for the EO-PVA sample. By comparing Fig. 5 with Fig. 1, it is found that the experimental results for the MY-PMMA and EO-PVA samples are consistent with the theoretical curves of case (a) and case (b), respectively, which reflects the fact that the value of A_1 in case (a) is more than that in case (b) for the same I_1.

The mechanism of the biphotonic holographic grating formation is different from that of one-photonic gratings. The biphotonic holographic grating can be attributed to the redistribution of the *cis* isomers of the azo molecules induced by the excitation of both the 633-nm light and the Hg light. In our experiment, the sample without irradiation of the Hg light cannot directly absorb the long-wavelength light to form the grating because at room temperature the azo molecules in the films exist mainly in the *trans* form, of which the absorptive band lies in the short-wavelength region. However, the Hg light used in the experiment can isomerize the *trans* isomers of the azo molecules to the *cis* form, which absorbs the long-wavelength light as presented in Fig. 3. When two intense 633-nm HeNe laser beams interfere in the sample, the spatial intensity modulation of the 633-nm light induces the $cis \rightarrow trans$ photoisomerization to be modulated as well, although the $trans \rightarrow cis$ photoisomerization is uniform by the irradiation of the noncoherent Hg light. As a result, the redistribution of the *cis* isomers forms a population grating, which diffracts the 633-nm reading beam.

B. Polarization properties of biphotonic holography

To confirm the mechanism of the biphotonic holographic grating and to compare with that of one-photon process, the polarization properties of the biphotonic holography are studied. At first, we investigate the effects of the polarizations of the long-wavelength light on the diffraction efficiency of biphotonic holography. Here the Hg light is not polarized, the three 633-nm beams have the equal intensity of 20 mW/cm^2 and have three different polarization configurations: (a) all *s* polarized, (b) beam I_c is *p* polarized and the others *s* polarized, (c) beam I_b is *p* polarized and the

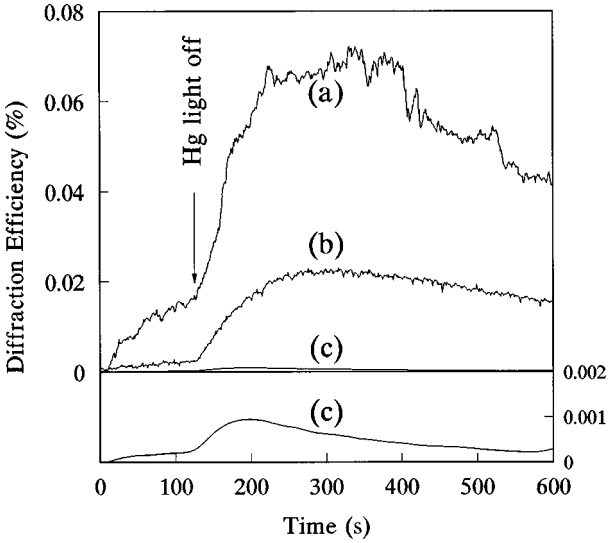

FIG. 6. Influence of polarization states of long-wavelength light on the diffraction efficiency of biphotonic holography. The Hg light has no polarization and three 633-nm beams have three polarization configurations: (a) all *s* polarized, (b) beam I_c is *p* polarized and the others *s* polarized, (c) beam I_b is *p* polarized and the others *s* polarized.

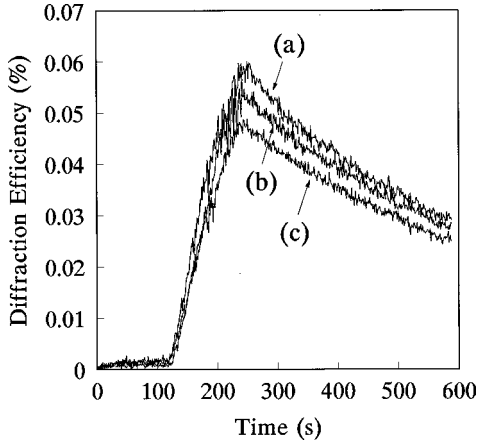

FIG. 7. Influence of polarization states of short-wavelength light on the diffraction efficiency of biphotonic holography. All 633-nm lights are *s* polarized, the short-wavelength light (i.e., 488-nm Ar^+ light) is (a) *s* polarized, (b) circular polarized, (c) *p* polarized.

others *s* polarized. The experimental results are shown in Fig. 6. It is found that curve (a) is more intense than curve (b), and that curve (c) is weakest and its intensity is almost zero. These results are distinct from that of one photon process, in which the signal is also very intense when the polarization state of writing beams is orthogonal.[33] Unlike the *trans* form of the azo molecule, the *cis* form has a planar structure and its permanent electric dipole moment can be negligible, so the polarization modulation of the writing interference field cannot form a nonisotropic grating, and only the intensity modulation can induce a population grating. In case (a) here, two population gratings can be formed in the sample by beam I_a interfering with beam I_b and by beam I_b interfering with beam I_c. However, there is just one population grating to be formed in case (b) because only the interference between beam I_a and beam I_b results in the light intensity modulation. Consequently, the signal in case (a) is more intense than that in case (b). In case (c), due to the orthogonal linear polarization between beam I_a and beam I_b as well as between beam I_b and beam I_c, there is no population grating to be formed. Therefore, there is no obvious diffraction signal to be observed.

The influence of the short-wavelength light polarization on the biphotonic holographic grating is also investigated. Since the Hg light is too weak after passing a polarizer, we adapt a 488-nm Ar^+ laser as the short-wavelength light to excite the sample. The intensity of the Ar^+ laser is fixed at 40 mW/cm^2, and three polarization states are studied: (a) *s* polarized, (b) circular polarized, and (c) *p* polarized. Three HeNe lasers are all *s* polarized with the intensity of 20 mW/cm^2 in each beam. Figure 7 shows that the polarization states of the Ar^+ laser do not affect the signal intensity notably. In other words, the reorientation of the *trans* isomers of the azo molecules induced by the polarized short-wavelength light does not influence the formation of biphotonic holographic grating significantly. The signal in case (a) is slightly stronger than that in others and in case (c) the signal is weakest. The reason is that the *trans* isomers with a strong polarization-selected absorption tend to align themselves to the direction perpendicular to the polarization of the short-wavelength light (488-nm laser) after the isomerization of $trans \leftrightarrow cis$ reaches its equilibrium. Thus, many more *cis* isomers have to populate in the direction parallel to the polarization of the short-wavelength light, although the electric dipole moment of the *cis* form is very weak. If the polarization of the writing light is the same as the short-wavelength light, the *cis* isomers absorb the writing light efficiently to form the grating. Hence, the diffraction efficiency of biphotonic holography in case (a) is slightly higher than the others. This experimental result confirms again that the biphotonic holographic grating is due to the population distribution of the *cis* isomers.

V. CONCLUSION

We have studied theoretically and experimentally the transient properties of the biphotonic holographic grating in the *trans-cis* isomerizative materials. The mechanism of the biphotonic holographic grating in azo materials can be attributed to the redistribution of the *cis* isomers induced by the excitations of both the short-wavelength and the long-wavelength lights. This model may also be suitable for other photoisomerizative (or photochromic) materials, such as spiropyran,[32,34] bacteriorhodopsin,[35] norbornadiene,[36] etc. The theoretical description reveals that the biphotonic holographic gratings will reach saturation under the irradiation of two color lights and will emerge a peak after the irradiation of the short-wavelength light stops. The condition of the occurrence of the maximum diffraction of the saturated grating and the dynamic evolution regularities of the diffraction peak are also demonstrated by the theory. The experimental results on the transient behaviors of biphotonic holography in the MY-PMMA film and the EO-PVA film agree well with the theoretical descriptions. The polarization properties of the biphotonic holography are studied, and it is found that the signal intensity of the biphotonic holography is influenced strongly by the polarization configurations of the long-

wavelength lights but only slightly by the polarization states of the short-wavelength light. These results further confirm that the biphotonic holography originates from the population grating of the *cis* isomers. This mechanism is different from that of one photonic process. The biphotonic grating discussed here may not only be used in photonic devices, such as optical memory, optical computing, and image processing elements, but may also be useful to study the mechanism of the isomerization process and to obtain the information about molecular characters of isomers.

*Author to whom correspondence should be addressed.
†Present address: School of Chemistry and Biochemistry, Georgia Institute of Technology, Atlanta, GA 30332.

[1] D. Dantsker, J. Nonlinear Opt. Phys. Mater. **5**, 775 (1996).
[2] D. Dantsker and S. Speiser, Appl. Phys. B: Lasers Opt. **58**, 97 (1994).
[3] Pengfei Wu, Wenju Chen, Xiong Gong, Guilan Zhang, and Guoqing Tang, Opt. Lett. **21**, 429 (1996).
[4] Alan G. Chen and D. J. Brady, Opt. Lett. **17**, 441 (1992).
[5] M. Ivanov, T. Todorov, L. Nikolova, N. Tomova, and V. Dragostinova, Appl. Phys. Lett. **66**, 2174 (1995).
[6] N. C. R. Holme, P. S. Ramanujam, and S. Hvilsted, Appl. Opt. **35**, 4622 (1996).
[7] Z. Sekkat, J. Wood, and W. Knoll, J. Opt. Soc. Am. B **14**, 829 (1997).
[8] P. S. Ramanjam, N. C. R. Holme, and S. Hvilsted, Appl. Phys. Lett. **68**, 1329 (1996).
[9] R. H. Berg, S. Hvilsted, and P. S. Ramanujam, Nature (London) **383**, 505 (1996).
[10] I. V. Tomov, T. E. Dutton, B. Vanwonterghem, and P. M. Kentzepis, J. Appl. Phys. **70**, 36 (1991).
[11] V. Fleurov, D. Brown, and C. Lawson, J. Nonlinear Opt. Phys. Mater. **6**, 95 (1997).
[12] Z. Sekkat, J. Wood, E. F. Aust, W. Knoll, W. Volksen, and R. D. Miller, J. Opt. Soc. Am. B **13**, 1713 (1996).
[13] G. G. Malliaras, V. V. Krasnikov, H. J. Bolink, and G. Hadziioannou, Appl. Phys. Lett. **67**, 455 (1995).
[14] N. C. R. Holme, P. S. Ramanujam, and S. Hvilsted, Appl. Opt. **35**, 4622 (1996).
[15] B. Fleck, H. Rehn, and L. Wenke, Proc. SPIE-Int. Soc. Opt. Eng. **2248**, 446 (1994).
[16] D. Psaltis, M. Levene, A. Pu, and G. Barbastathis, Opt. Lett. **20**, 782 (1995).
[17] Y. Shi, W. H. Steier, L. Yu, M. Chen, and L. R. Dalton, Appl. Phys. Lett. **59**, 2935 (1991).
[18] X. Tong, A. Yariv, M. Zhang, A. J. Agranat, R. Hofmeister, and V. Leyva, Appl. Phys. Lett. **70**, 2241 (1997).
[19] Jean J. A. Couture, Appl. Opt. **30**, 2858 (1991).
[20] Z. Sekkat, J. Wood, E. F. Aust, W. Knoll, W. Volksen, and R. D. Miller, J. Opt. Soc. Am. B **13**, 1713 (1996).
[21] R. A. Hill, S. Dreher, A. Dreher, A. Knoesen, and D. R. Yankelevich, Appl. Phys. Lett. **66**, 2156 (1995).
[22] T. Kaino and S. Tomaru, Adv. Mater. **5**, 172 (1993).
[23] W. Nie, Adv. Mater. **5**, 520 (1993).
[24] P. Rochon, J. Gosselin, A. Natansohn, and S. Xie, Appl. Phys. Lett. **60**, 4 (1992).
[25] D. Y. Kim, L. Li, R. J. Jeng, J. Kumar, M. A. Fiddy, and S. K. Tripathy, Proc. SPIE-Int. Soc. Opt. Eng. **1853**, 23 (1993).
[26] P. Rochon, E. Batalla, and A. Natansohn, Appl. Phys. Lett. **66**, 136 (1995).
[27] D. Y. Kim, S. K. Tripathy, L. Li, and J. Kumar, Appl. Phys. Lett. **66**, 1166 (1995).
[28] N. C. R. Holme, L. Nikolova, P. S. Ramanujam, and S. Hvilsted, Appl. Phys. Lett. **70**, 1518 (1997).
[29] C. J. Barrett, A. L. Natansohn, and P. L. Rochon, J. Phys. Chem. **100**, 8836 (1996).
[30] N. Tamaoki, S. Yoshimura, and T. Yamaoka, Thin Solid Films **221**, 132 (1992).
[31] J. F. Rabek, *Photochemistry and Photophysics* (CRC, Boca Raton, FL, 1990), pp. 120–141.
[32] V. Weiss, A. A. Friesem, and V. A. Kronganz, Opt. Lett. **18**, 1089 (1993).
[33] C. Egami, K. Nakagawa, and H. Fujiwara, Jpn. J. Appl. Phys., Part 1 **31**, 2937 (1992).
[34] R. M. Tarkka, M. E. Talbot, D. J. Brady, and G. B. Schuster, Opt. Commun. **109**, 54 (1994).
[35] A. Lewis, Y. Albeck, Z. Lange, J. Benchowski, and G. Weizman, Science **275**, 1462 (1997).
[36] K. Kinoshita, K. Horie, S. Morino, and T. Nishikubo, Appl. Phys. Lett. **70**, 2940 (1997).